

RESEARCH ARTICLE

Fabrication of a guar gum-based composite hydrogel for brilliant green dye adsorption

Haider M. Musa^{1*}, Nadher D. Radia²

¹ Ministry of Education, General Directorate of Education of Babylon, Babylon, Iraq

² Department of Chemistry, College of Education, University of Al-Qadisiyah, Al-Qadisiyah, Iraq

*Corresponding author: Haider M. Musa, edu.chem.post24.4@qu.edu.iq

ABSTRACT

Brilliant Green (BG), a triphenylmethane dye with high chemical stability, represents a significant source of environmental concern due to its recalcitrance to degradation and the difficulty of its removal using conventional industrial wastewater treatment methods. In response to these challenges, a novel composite hydrogel adsorbent, designated as Guar gum-grafted poly(Acrylic Acid-co-Sodium 4-vinylbenzenesulfonate GG-g-poly (AAc-NaVBS)/AC, was developed. This was achieved through the graft copolymerization of acrylic acid (AAc) and Sodium 4-vinylbenzenesulfonate (NaVBS) onto a natural guar gum (GG) backbone, coupled with the incorporation of activated carbon (AC) to enhance its surface properties and porosity. The structural and morphological properties of the hydrogel composite were characterized using Fourier-transform infrared spectroscopy (FTIR), X-ray diffraction (XRD), and scanning electron microscopy (SEM), in addition to determining its point of zero charge (pHpzc). The results revealed that the prepared material possesses a highly porous structure and active functional groups, which contributed to achieving a maximum adsorption capacity of 820.9 mg/g at temperature of 25 °C. The adsorption kinetics study indicated that the process followed the pseudo-second-order kinetic model. Furthermore, the equilibrium data showed a good fit with the Freundlich isotherm model, indicating a multilayer adsorption process on a heterogeneous surface with moderate adsorbent-adsorbate interactions. Additionally, the hydrogel composite demonstrated excellent reusability over several adsorption-desorption cycles without significant deterioration in performance, supporting its potential for long-term industrial applications in water treatment. This study highlights the efficacy of integrating natural polymers with functional materials to develop eco-friendly and highly efficient adsorbents for the removal of complex organic pollutants from various aqueous systems.

Keywords: Activated Carbon, Hydrogel; Brilliant Green dye; Guar Gum; Adsorption; Kinetic Models; Isotherm Models

ARTICLE INFO

Received: 1 August 2025

Accepted: 2 September 2025

Available online: 10 September 2025

COPYRIGHT

Copyright © 2025 by author(s).

Applied Chemical Engineering is published by Arts and Science Press Pte. Ltd. This work is licensed under the Creative Commons Attribution-NonCommercial 4.0 International License (CC BY 4.0).

<https://creativecommons.org/licenses/by/4.0/>

1. Introduction

The depletion of potable water resources, resulting from the indiscriminate disposal of untreated industrial effluents into water bodies, is one of the most pressing contemporary environmental challenges. Over the past few decades, numerous industrial sectors have exacerbated this problem by discharging a variety of pollutants, including dyes, heavy metals, and chemical compounds, thereby necessitating specialized scientific research in this field. Dyes are widely used in several industries, such as textiles, paper, and leather manufacturing. However, their improper disposal can lead to adverse effects on humans and aquatic organisms, in addition to degrading the aesthetic quality of water bodies. Dyes reduce light penetration in water, which impairs the photosynthetic efficiency of aquatic plants and organisms^[1, 2]. This leads to a decrease in the dissolved oxygen

concentration, threatening aquatic life. Furthermore, some dyes contain toxic components, such as heavy metals, which can bioaccumulate in the human body and cause severe health issues, including carcinogenesis, respiratory disorders, and skin irritation. Dyes are considered hazardous pollutants that can cause significant harm to the environment and public health, making their effective removal from industrial wastewater essential. These pollutants also alter the color and odor of water, negatively impacting its aesthetic and economic value. Therefore, the removal of dyes from wastewater is a crucial step before its discharge into the environment, which can be achieved using effective treatment technologies like membrane filtration, adsorption, coagulation, and flocculation to mitigate their environmental and health impacts. Industrial dyes also contribute to reducing the solubility of gases in water, which impairs the oxygen reaeration process and can lead to the development of a harmful anaerobic environment. Among these dyes, Brilliant Green (BG) is considered one of the most hazardous^[3-5]. It is a synthetic cationic dye used in various applications, including the coloring of paper, silk, wool, rubber, and leather, as well as in some veterinary applications and as an intestinal parasiticide. The direct discharge of BG dye into water bodies poses a significant threat to aquatic life and human health, mandating its effective treatment prior to disposal. Numerous methods have been developed for the removal of dyes from industrial wastewater, including membrane separation, coagulation-precipitation, advanced oxidation, biological treatment, photocatalysis, electrocoagulation, adsorption, and electrochemical treatments. Among these, adsorption is one of the most widely used and effective methods due to its operational simplicity, high efficiency, low cost, and broad applicability. The efficiency of this method largely depends on selecting a suitable adsorbent material characterized by high adsorption capacity, ease of preparation, chemical stability, reusability, and low cost. A variety of materials have been used as adsorbents for dye removal, including activated carbon, composites, zeolites, clay minerals, and polymers, as well as natural materials like biochar and other biosorbents^[6-9]. Guar gum (GG) is a water-soluble natural polymer composed of a linear mannan backbone randomly branched with galactose units at an approximate 2:1 ratio. Its molecular chains contain numerous hydroxyl (-OH) groups that impart unique properties. Due to its high molecular weight and abundance of functional groups, it can be directly used for the removal of heavy metal ions from water. The hydroxyl groups in its structure also facilitate the modification of its properties through reactions with organic molecules or vinyl monomers, leading to the production of materials with enhanced functional characteristics. Moreover, GG or its derivatives can be combined or modified with other polymers or nanomaterials to create hydrogel composite s with higher efficiency in pollutant removal. Hydrogel composite s are materials characterized by a three-dimensional (3D) network structure capable of absorbing and retaining large amounts of water or aqueous fluids, often many times their dry weight. They are produced from the reaction of swellable monomers, and the fluid is retained due to the hydrophilic functional groups along the polymer chain^[10, 11]. The swelling nature of these hydrogel composites, along with advantages such as biocompatibility, mechanical behavior, and surface properties, enhances their effectiveness. They are also environmentally friendly materials used in numerous applications, including wastewater treatment. Researchers have shown increasing interest in developing and applying nanomaterials by incorporating them into polymer matrices due to their significant impact on enhancing the mechanical properties of biopolymers. AC is another highly efficient material for pollutant removal, owing to its distinctive properties like high porosity and large specific surface area. Its effectiveness depends on the precursor material, activation method, and surface chemistry. It can be produced from various sources, such as agricultural waste, fruit residues, and low-grade coal. Although low-grade coal, such as Malaysian coal, is unsuitable for power generation, it can be converted into highly efficient AC through appropriate processing, making it an economical and effective option for water purification and other environmental applications^[11-14].

This study involved the preparation, characterization, and application of a novel hydrogel composite. GG was integrated with AC within a three-dimensional polymeric network. The synthesis was performed using cross-linkable monomers to form a hydrogel effective in the adsorption of BG dye from aqueous solutions. The prepared hydrogel composite demonstrated high efficiency in dye removal, and its performance was

evaluated under various operational parameters, including contact time, temperature, initial pH, ionic strength, and the point of zero charge .

2. Materials and methods

2.1. Materials

Guar gum (GG, 99% purity), activated carbon (AC, commercial grade, Macklin, China; BET surface area $\approx 33.4 \text{ m}^2/\text{g}$, average pore diameter $\approx 3.2 \text{ nm}$, and crystallite size $\approx 28 \text{ nm}$), and Brilliant Green (BG, 99% purity) dye were obtained from Macklin, China. Acrylic acid (AAc, 99% purity) and potassium persulfate (KPS, 99% purity) were purchased from SRL, India. N,N'-methylenebisacrylamide (MBA, 98% purity), sodium hydroxide (NaOH, 99% purity), hydrochloric acid (HCl, 37%), calcium chloride (CaCl_2 , 99% purity), and sodium 4-vinylbenzenesulfonate (NaVBS, 90% purity) were also supplied by Macklin. All chemicals were of analytical grade and used directly without further purification. Deionized water was employed for all preparations and experimental procedures.

2.2. Method

To determine the optimum activated carbon (AC) loading, varying amounts of AC (0.0125, 0.025, 0.05, and 0.075 g) were dispersed in 2 mL of distilled water and subjected to ultrasonication for 1 h to ensure uniform dispersion. In a separate beaker, 0.1 g of guar gum (GG) was dissolved in 30 mL of distilled water under constant magnetic stirring until a homogeneous solution was obtained. The AC suspension was then gradually added to the GG solution under a continuous nitrogen purge to prevent premature oxidation. Subsequently, 0.04 g of N,N'-methylene-bisacrylamide (MBA, crosslinker) dissolved in 2 mL of distilled water was added, followed by 0.04 g of potassium persulfate (KPS, initiator) dissolved in 2 mL of water. Acrylic acid (AAc) was introduced as the primary monomer, along with 0.2 g of sodium 4-vinylbenzenesulfonate (NaVBS) to enhance hydrophilicity and charge density. The final reaction mixture was transferred into test tubes and placed in a water bath at 70°C for 4 h to complete the polymerization process. After polymerization, the resulting hydrogel was cut into small pieces and repeatedly washed with distilled water at 1 h intervals for 6 h to remove residual monomers, initiators, and crosslinkers. The washed samples were then soaked in ethanol for 24 h to further eliminate unreacted species. Finally, the product was dried in an oven at 70°C to a constant weight and ground into a fine, homogeneous powder, as depicted in **Figure 1**. Among the tested dosages, 0.05 g AC was identified as the optimum loading, as it provided the highest adsorption performance while maintaining structural integrity of the hydrogel network.

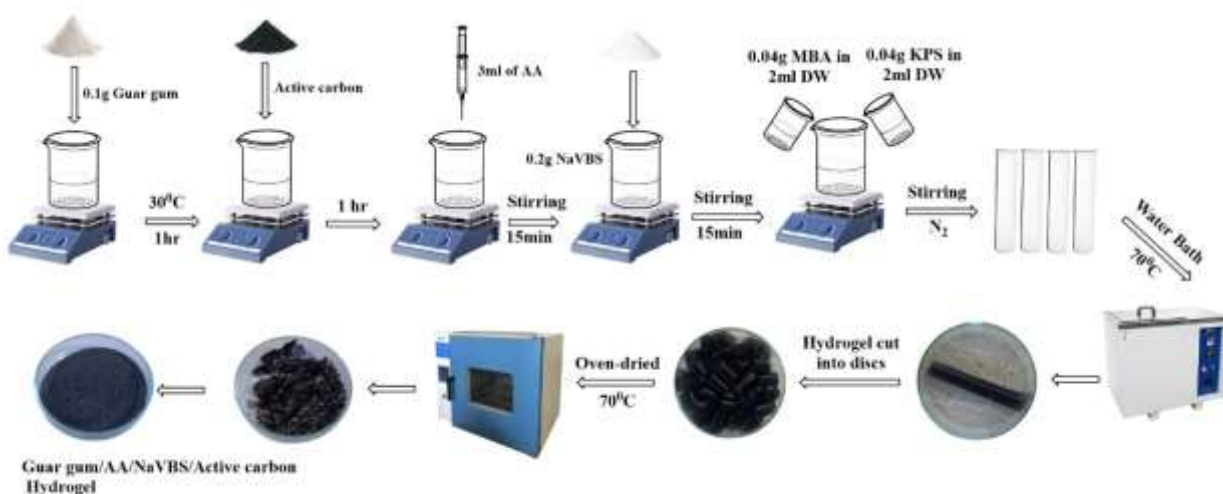


Figure 1. Preparation of GG-g-poly (AAc-NaVBS)/AC hydrogel composite

2.3. Batch adsorption process

Adsorption experiments were conducted using BG dye as a model for industrial dye pollutants in water. To determine the equilibrium time, 0.006 g of the composite hydrogel was mixed with 10 mL of a 500 ppm BG dye solution. The mixture was agitated in a shaker at 120 rpm at a constant temperature of 25°C. Aliquots were withdrawn at various time intervals over a 180 min period. The results showed that equilibrium was achieved within 60 min. The absorbance of the solutions was measured using a UV-Vis spectrophotometer at the λ_{max} of 624 nm. The effect of temperature on adsorption was investigated at 15, 25, and 35°C. the same adsorbent dosage 0.006 g was added to 10 mL of BG dye solutions with varying initial concentrations (400–1000 ppm). The samples were agitated for the equilibrium time of 60 min, after which the mixtures were centrifuged and the absorbance of the supernatant was measured. To evaluate the effect of pH, the initial pH of the dye solutions was adjusted (3- 10) using NaOH (0.1 M) and HCl (0.1 M). Then, 0.006 g of the adsorbent was added to 10 mL of a 500 ppm dye solution. The samples were incubated at 25°C for 1 h before measurement. The effect of ionic strength was studied by adding various amounts of NaCl and CaCl₂ salts (0.001 - 0.05 g) to the dye solution along with 0.006 g of the adsorbent. The samples were agitated for 60 min at 25°C, after which the absorbance was measured.

The adsorption capacity, Q_e was calculated using the following equation:

$$Q_e = ((C_0 - C_e) \times V) / m \quad (1)$$

The removal efficiency was calculated using the equation:

$$\% \text{ Removal} = ((C_0 - C_e) / C_0) \times 100 \quad (2)$$

Where: C_0 : Initial dye concentration (mg/L), C_e equilibrium dye concentration (mg/L), V volume of the solution (L), m : mass of the adsorbent (g) and q_e : Adsorption capacity at equilibrium (mg/g).

To evaluate the performance of the hydrogel composite in removing BG dye from aqueous solutions, the adsorption data were analyzed using three of the most widely used isotherm models. These models aim to describe the adsorption behavior through mathematical relationships that link the amount of adsorbate to influential factors. They also help in understanding the nature of the interaction between the composite and the dye molecules:

1. Langmuir Isotherm Model

$$Q_e = \frac{Q_m \cdot K_L \cdot C_e}{1 + K_L \cdot C_e} \quad (3)$$

Where: Q_m : maximum adsorption capacity (mg/g), K_L : Langmuir constant (L/mg), and indicating the affinity of the binding sites and.

2. Freundlich Isotherm Model

$$Q_e = K_f C_e^{\frac{1}{n}} \quad (4)$$

Where: K_f : Freundlich constant related to adsorption capacity, and $1/n$: Freundlich exponent indicating adsorption intensity.

3. Temkin Isotherm Model

$$Q_e = B \ln(K_T \cdot C_e) \quad (5)$$

Where: B : Constant related to adsorption heat (mg/g), and K_T : Temkin equilibrium binding constant (L/g).

2.4. Reusability study

The hydrogel composite was regenerated by washing it in a 0.1 M HCl solution using a shaker for more than 4 h. After acid treatment, it was thoroughly rinsed with distilled water until a neutral pH was achieved

and then dried. The regenerated composite was reused in subsequent adsorption experiments, and the results showed that it retained good efficiency after multiple cycles, confirming its suitability for repeated use in dye removal applications.

2.5. Point of Zero Charge (pHpzc)

The point of zero charge (pHpzc) was determined using the pH drift method. A series of 500 ppm NaCl solutions were prepared, and their initial pH (pH_i) was adjusted to values (2-12) by NaOH (0.1 M) and HCl (0.1 M). A 0.007 g of the hydrogel composite was added to 20 mL of each solution. The mixtures were then agitated for 24 h at 25°C to reach equilibrium. The final pH (pH_f) of each solution was measured. The pHpzc is the point where the plot of ΔpH ($\Delta pH = pH_i - pH_f$) versus pH_i crosses the line at $\Delta pH = 0$.

2.6. Swelling ratio

The swelling behavior of the hydrogel composite was analyzed across a pH (2-10). Accurately weighed dry samples were immersed in solutions of different pH values and incubated for a sufficient period at room temperature. After reaching swelling equilibrium, the samples were removed, blotted gently to remove excess surface water, and weighed.

The swelling ratio (%) was calculated using the following equation:

$$\text{Swelling (\%)} = (W_s - W_i / W_i) \times 100 \quad (6)$$

Where W_s : weight of the swollen sample, and W_i Weight of the dry sample

3. Results and discussion

3.1. FTIR Analysis

The FT-IR spectra of AC, GG, hydrogel, and the hydrogel composite reveal key structural differences. A broad O–H/N–H band (3600–3000 cm^{-1}) dominates in GG and the hydrogel systems, indicating rich hydroxyl content and hydrogen bonding, while AC shows weaker OH groups. The hydrogel exhibits a strong C=O peak ($\sim 1730 \text{ cm}^{-1}$), reflecting introduced carbonyl/amide functionalities, which in the composite shift slightly due to interaction with AC^[15]. The band at 1650–1600 cm^{-1} arises from water bending in hydrogels and aromatic C=C stretching in AC. The symmetric COO^- stretch (1450–1410 cm^{-1}) is more pronounced in the composite, suggesting ionized carboxyls involved in interfacial bonding. Strong glycosidic C–O–C/C–O vibrations (1150–1020 cm^{-1}) confirm the GG backbone, with slight shifts in the hydrogel and composite, indicating crosslinking and polymer–AC integration. Overall, the composite spectrum shows both GG/hydrogel signatures and AC-related aromatic features, highlighting synergistic interactions.^[16, 17] As shown **Figure 2a**.

comparing the composite before and after adsorption shows clear functional group involvement in binding. The O–H/N–H band (3600–3000 cm^{-1}) becomes broader and more red-shifted after adsorption, evidencing stronger hydrogen bonding. The C=O peak ($\sim 1730 \text{ cm}^{-1}$) decreases and shifts, while COO^- bands (1450–1410 cm^{-1}) increase, confirming participation of carbonyl and carboxylate groups in complexation. Enhanced intensity near 1650–1600 cm^{-1} suggests additional aromatic or amide contributions from the adsorbate. Meanwhile, subtle changes in saccharide C–O/C–O–C bands (1200–1000 cm^{-1}) indicate that hydroxyls in the polysaccharide matrix are also active in binding. Altogether, adsorption proceeds through multi-site interactions: hydrogen bonding, electrostatic/coordination via carboxyls, and possible π – π interactions with AC's aromatic surface^[18, 19]. As shown **Figure 2a**.

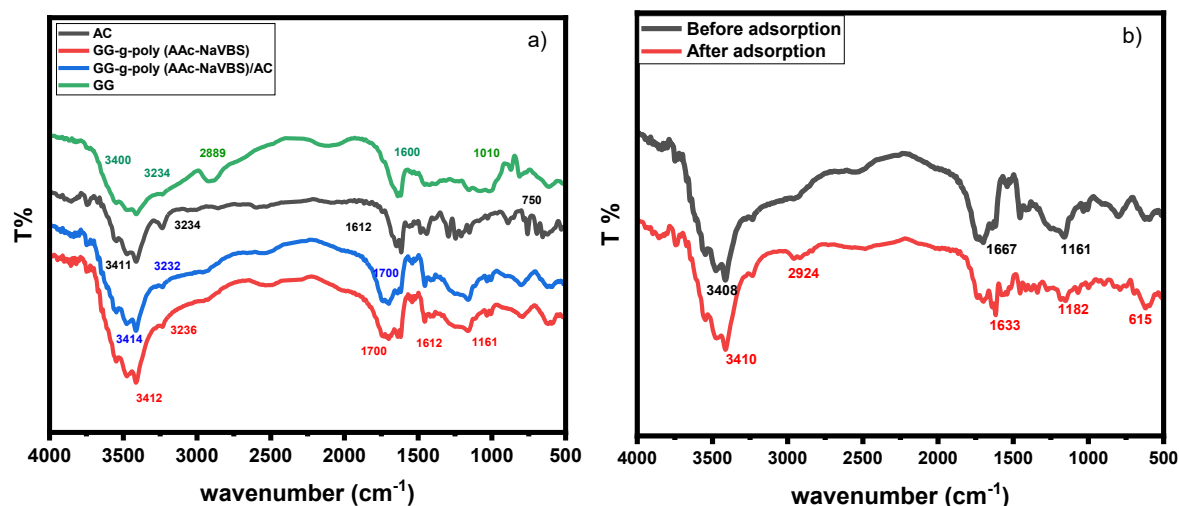


Figure 2. FTIR spectra of: (a) AC, hydrogel, hydrogel composite, GG; and (b) The hydrogel composite before and after the adsorption of BG dye

3.2. X-ray diffraction analysis

The X-ray diffraction (XRD) technique was employed to analyze the structural characteristics of the materials used in the hydrogel composite, with the objective of evaluating whether they possessed an ordered crystalline or an amorphous structure. The XRD patterns for the samples GG, AC, hydrogel, and hydrogel composite are illustrated in the **Figure 3**. The spectrum of GG reveals a broad diffraction halo within the 2θ range of $10\text{--}30^\circ$, with no distinct peaks. This indicates the amorphous nature of the material, which is attributed to its being a natural polymer with a random structure that lacks regular crystalline order. Meanwhile, the activated carbon spectrum displays weak and irregular peaks in the $2\theta = 10\text{--}50^\circ$ range, reflecting limited ordering in some regions of the sample. Consequently, it is classified as a semi-amorphous material with a partially ordered structure. As for the hydrogel spectrum, it is characterized by a more defined diffraction halo spanning approximately from $2\theta = 15\text{--}40^\circ$. This pattern is ascribed to the cross-linking of the polymer chains, which imparts a partially amorphous nature to the material^[20].

In the case of the hydrogel composite spectrum, it exhibits sharper and more defined peaks within the $2\theta = 15\text{--}35^\circ$ range compared to the other samples. This suggests a notable improvement in the internal organization resulting from the structural interaction between guar gum, activated carbon, and the hydrogel network. This led to the material's transformation from an amorphous to a semi-crystalline structure, which confirms the success of the hydrogel composite structural preparation **Figure 3**.

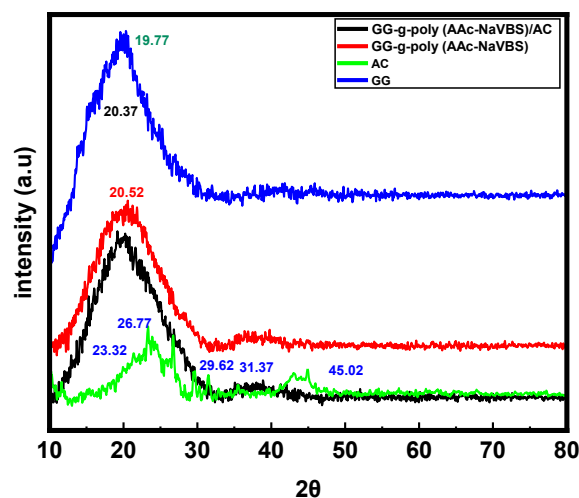


Figure 3. XRD patterns of the GG, AC, hydrogel, and hydrogel composite

3.3. Scanning Electron Microscopy (SEM)

SEM was utilized to study the morphological changes in the surface structure of both the prepared hydrogel and the GG-g-poly (AAc-NaVBS)/AC hydrogel composite, before and after the adsorption of BG dye. The objective was to evaluate the effect of incorporating activated carbon and the efficacy of the adsorption process. SEM images of the hydrogel, as illustrated in **Figure 4a**, revealed that the surface is characterized by a spongy structure composed of interconnected layers and distinct porosity. A flaky surface appearance with slight topographical features, resulting from the cross-linking of polymer chains by the cross-linking agent (MBA), was also observed. The surface is also noted to be relatively smooth with irregularly distributed wrinkles, reflecting an open polymeric nature capable of readily accommodating molecules during adsorption. Following the incorporation of activated carbon into the hydrogel network to form the hydrogel composite, as shown in **Figure 4b**, prominent changes in the surface morphology occurred. The surface became rougher, the degree of porosity increased, and the structure became more irregular. These changes can be attributed to the homogeneous distribution of activated carbon particles within the polymeric matrix. This is a result of the interaction between the functional groups on the activated carbon surface (such as $-\text{OH}$ and $-\text{COOH}$) and the polymer chains, alongside the influence of van der Waals forces, which effectively aided in immobilizing the particles within the hydrogel composite structure [21, 22].

After the adsorption of BG dye, as depicted in **Figure 4c**, the surface was observed to be smoother and more homogeneous, with a distinct reduction in the number of visible pores compared to its previous state. This change is ascribed to the penetration of dye molecules into the available pores and their subsequent filling, which resulted in the partial or complete coverage of the hydrogel composite surface by dye molecules. These changes in surface appearance serve as a clear visual indicator of the successful adsorption process, reflecting the effective interaction between the material's surface and the pollutant molecules. Collectively, these findings indicate that the hydrogel composite possesses an active and effective surface structure, capable of efficiently accommodating BG dye molecules, which reinforces its potential for environmental remediation applications [23, 24]

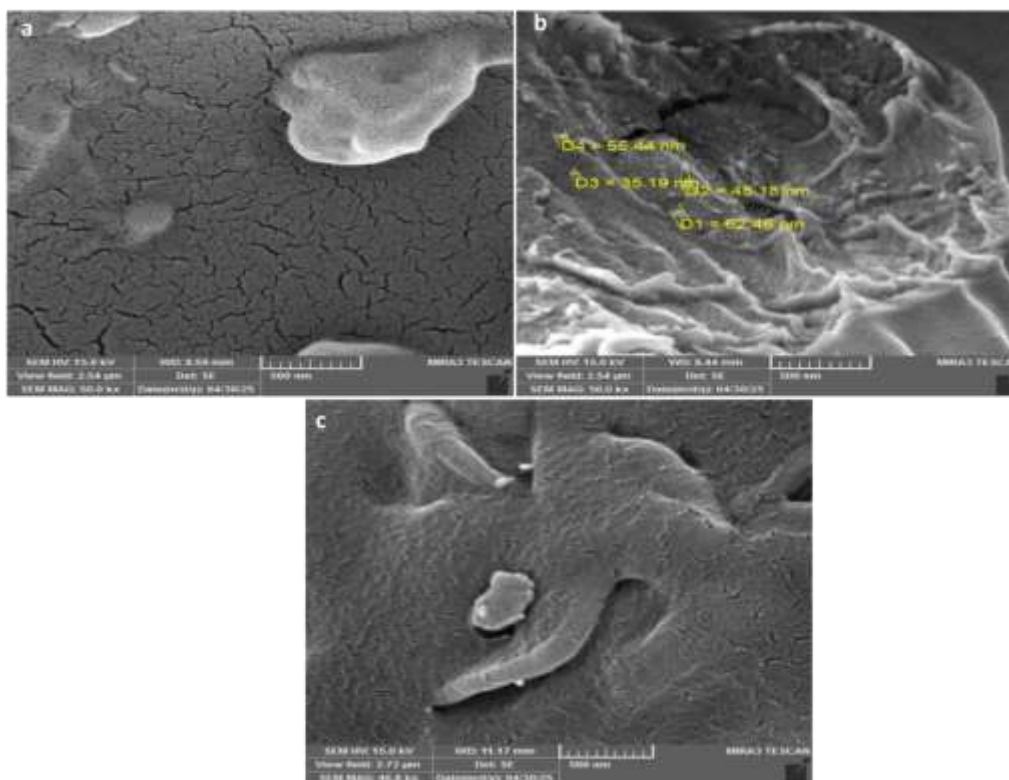


Figure 4. SEM images of: (a) hydrogel, (b) hydrogel composite, and (c) hydrogel composite after adsorption of BG dye

3.4. Point of zero charge

The point of zero charge (pHpzc) is a fundamental surface property of an adsorbent material, representing the pH value at which the net surface charge of the material is zero. Under this condition, all active sites are electrically neutral, exhibiting no preference for carrying a positive or negative charge. The determination of the pH < pH pzc is critically important for interpreting adsorption behavior in solutions with varying pH values. As illustrated in **Figure 5**, the pH < pH pzc value for the prepared hydrogel was 4.548. In contrast, this value decreased to 4.226 in the GG-g-poly (AAc-NaVBS)/AC hydrogel composite after the incorporation of activated carbon. This indicates that integrating activated carbon into the hydrogel structure contributed to modifying the surface properties, leading to the acquisition of a negative charge over a broader pH range compared to the pristine hydrogel. At pH values above the pH < pH pzc, the adsorbent is negatively charged, whereas it becomes positively charged at pH values below this point. Since BG dye is a cationic species in an aqueous medium, the presence of a negative charge on the material's surface is a crucial condition for enhancing the adsorption process through electrostatic interactions.

Based on these results, the hydrogel composite possesses a greater tendency to develop a negatively charged adsorbent compared to the hydrogel, thereby enhancing its efficiency in attracting the positively charged BG dye under the prevailing conditions^[43]. This reflects the critical role of modifying the material's surface with activated carbon in improving its adsorption properties and broadening the acid-base response range of the surface^[8].

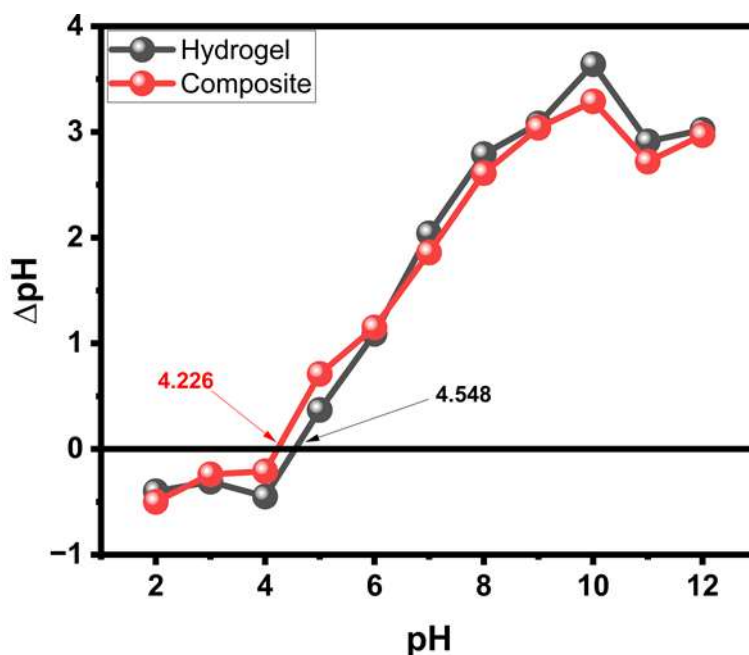


Figure 5. PHpzc of the hydrogel and hydrogel composite

3.5. Swelling analysis

The swelling ratio of both the hydrogel and the GG-g-poly (AAc-NaVBS)/AC hydrogel composite was investigated across a pH (2-10) as illustrated in **Figure 6**. The results revealed that the swelling ratio is markedly dependent on the acidic to basic solution. At pH values below 4, the ratio was low for both samples due to the protonation of functional groups (-COOH, -OH), which diminishes the electrostatic repulsion between polymer chains and thus restricts water uptake. Beginning at pH 6, the hydrogel composite outperformed the hydrogel, which is attributed to the role of activated carbon in increasing porosity and providing additional active sites. At pH 7, the hydrogel reached its peak swelling, whereas the hydrogel

composite maintained a very comparable performance, indicating that the carbon incorporation did not adversely impact its absorption capacity.

Under basic conditions pH 10, the swelling ratio decreased for both systems; however, the hydrogel composite sustained a superior performance, owing to its structural stability. These findings confirm that the incorporation of activated carbon improved the swelling properties, thereby enhancing the hydrogel composite efficacy in various environments^[25]

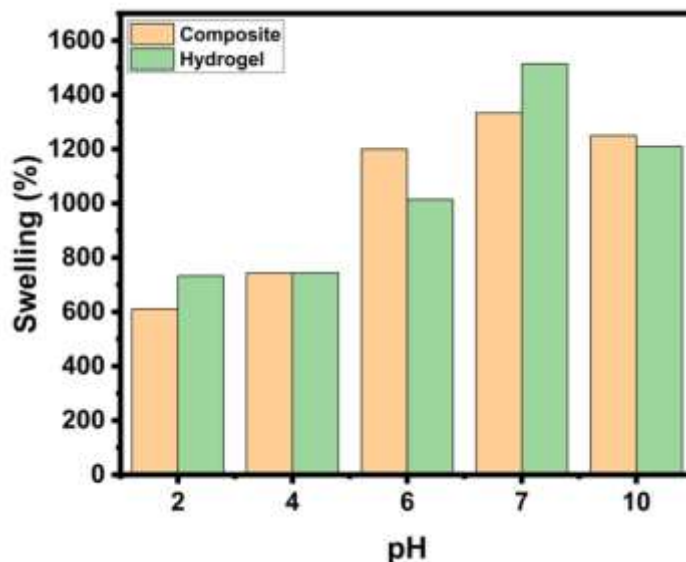


Figure 6. Swelling ratio of the hydrogel and hydrogel composite

3.6. Effect of adsorbent dosage

The influence of the adsorbent dosage (0.001-0.010 g) on the adsorption of BG dye was evaluated by measuring both the adsorption capacity (Q_e , mg/g) and the removal efficiency (R %), as depicted in Figure 7. The results showed that Q_e was highest at lower adsorbent dosage, at 0.001 g, and decreased progressively with increasing adsorbent dosage. This behavior is attributed to the constant dye concentration in solution, which leads to the distribution of dye molecules across a larger number of adsorption sites, thereby reducing the specific uptake per unit mass. Conversely, dye removal efficiency increased with hydrogel composite dosage, reaching a maximum at 0.006 g, and showed minimal variation at higher weights. This indicates that most effective adsorption sites had become saturated and that further increases in dosage did not significantly enhance performance^[26]

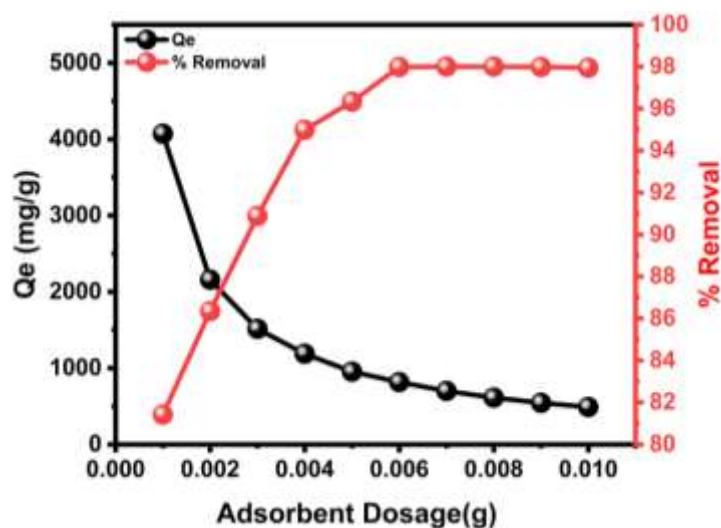


Figure 7. Effect of adsorbent dosage onto the adsorption of BG dye

3.7. Effect of contact time

The effect of contact time on the adsorption efficiency of BG dye by the hydrogel composite was investigated at a constant temperature of 25 °C, an adsorbent dosage of 0.006 g, and an initial dye concentration of 500 ppm, as depicted in **Figure 8**. The study encompassed contact times ranging from (3-180 min) to determine the equilibrium time. The results revealed that the adsorption process was rapid during the initial minutes, a phenomenon attributed to the high availability of unsaturated active sites on the adsorbent surface. As time progressed, the rate of adsorption gradually decreased due to the progressive saturation of the surface, until a state of equilibrium was established after 60 min. Consequently, a contact time of 60 min is considered optimal for reaching equilibrium, as it achieves the maximum adsorption efficiency within a practical operational timeframe. Further extension of the contact time beyond this point did not yield any significant improvement in performance^[22]

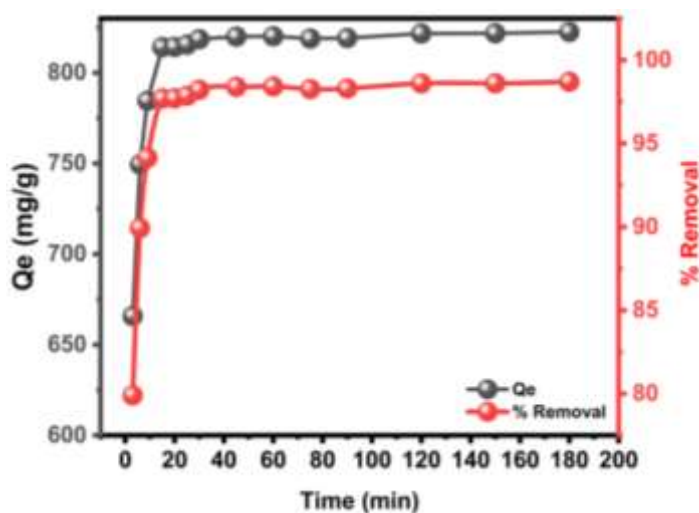


Figure 8. Effect of contact time on the adsorption of BG dye

3.8. Effect of pH

The solution pH plays a critical role in determining the adsorption efficiency of BG dye, owing to its direct influence on the surface charge of the hydrogel composite and the speciation of the dye molecules in the aqueous medium, as illustrated in **Figure 9**. At low pH values, the high concentration of H^+ leads to competition with the cationic dye molecules for the active adsorption sites. This results in a decreased adsorption efficiency. As the pH value increases, the functional groups on the hydrogel composite (such as $-COOH$ and $-OH$) undergo deprotonation, creating a net negative charge^[27]. This enhances the electrostatic attraction with the positively charged BG molecules, thereby increasing the quantity of adsorbed dye. Furthermore, the increased negative charge density induces repulsion between the polymer chains, leading to an expansion of the hydrogel network and an increased swelling ratio. This, in turn, facilitates the diffusion of dye molecules into the interior of the structure, contributing to an overall improvement in adsorption efficiency^[16, 17]

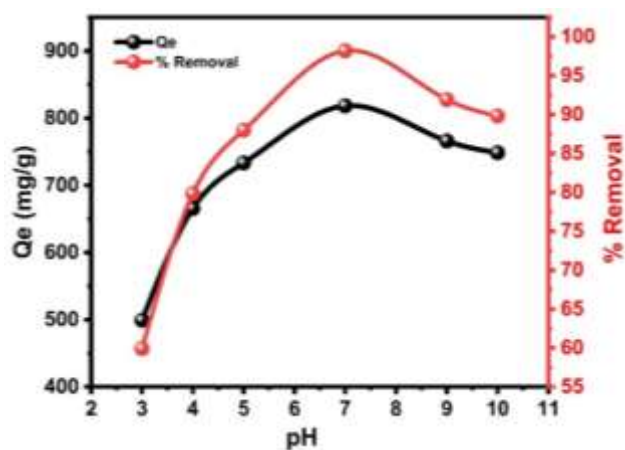


Figure 9. Effect of pH on the adsorption of BG dye

3.9. Effect of salts on the adsorption

As illustrated in **Figure 10**, the study demonstrated that an increase in the concentration of salts, such as NaCl and CaCl₂, in the adsorption leads to a pronounced decrease in the adsorption efficiency of BG dye onto the hydrogel composite. This decrease is attributed to the competitive effect between the cations (Na⁺ and Ca²⁺) and the positively charged BG molecules for the available active sites on the adsorbent surface. It was observed that the inhibitory effect of Ca²⁺ was more significant compared to that of Na⁺. This is due to its divalent charge, which enhances its ability to create electrostatic shielding, thereby diminishing the attractive forces between the hydrogel composite and the dye. The results indicate that salts, particularly those with divalent cations, significantly impair the adsorption efficiency. This highlights the necessity of controlling the ionic strength in practical systems to ensure effective treatment performance^[26].

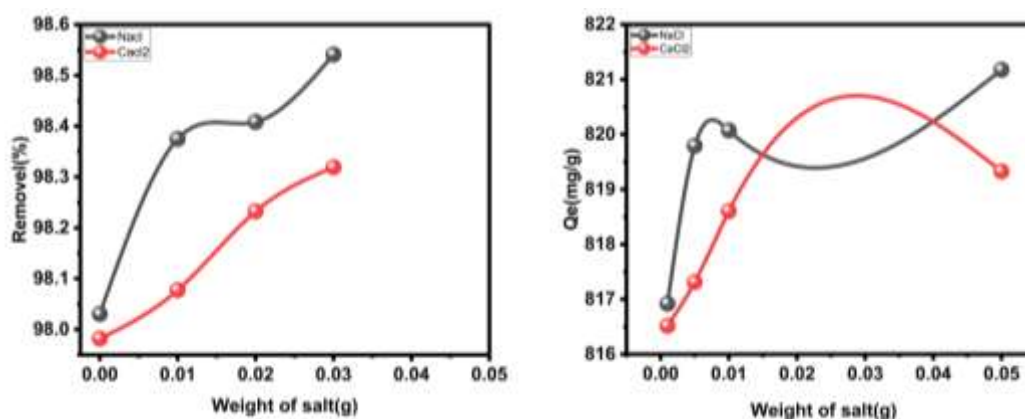


Figure 10. Effect of Salts on the Adsorption

3.10. Effect of temperature

The effect of temperature on the adsorption of BG dye was evaluated by examining the relationship between the equilibrium concentration (Ce) and the amount adsorbed at equilibrium (Qe) at 15, 25, and 35 °C, as illustrated in **Figure 11**. The results indicated that Qe increased with a rise in Ce under all temperatures. However, the adsorption efficiency was higher at lower temperatures, most notably at 15 °C, where Qe reached a value exceeding 140 mg/g, in contrast to the lower values observed at 25 and 35 °C. This behavior suggests that the adsorption process is exothermic in nature, as an increase in temperature diminishes the stability of the dye molecules on the material's surface, thereby weakening the adsorption forces. This can be attributed to the increased kinetic energy of the molecules, which promotes their desorption from the active surface. Consequently, operating at a lower temperature is a favorable condition for enhancing the dye removal efficiency^[24]

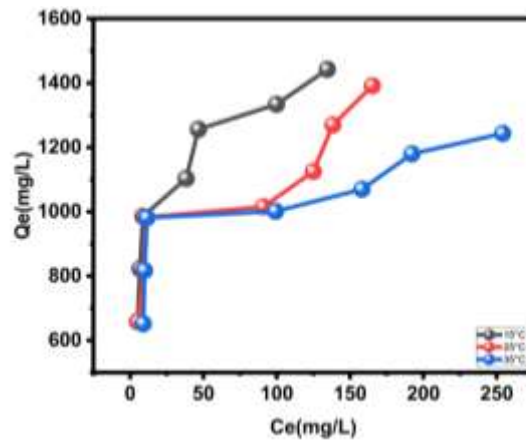


Figure 11. Effect of Temperature on the Adsorption

3.11. Adsorption isotherm models

The adsorption isotherm behavior of Brilliant Green (BG) dye onto the nanocomposite was evaluated using three classical models: Langmuir, Freundlich, and Temkin, at different temperatures (15, 25, and 35 °C), as illustrated in Figure 12. Although the Langmuir model exhibited a relatively high correlation at 15 °C ($Q_{\text{max}} = 1399.36 \text{ mg g}^{-1}$, $R^2 = 0.93$), its fitting accuracy decreased markedly with increasing temperature (R^2 dropping to 0.74 at 35 °C). In contrast, the Freundlich model provided consistently higher correlation coefficients across the studied temperatures ($R^2 = 0.92\text{--}0.76$), confirming that adsorption is better described by a heterogeneous multilayer process rather than a strictly homogeneous monolayer mechanism. The increase in the Freundlich constants (K_F and n) with rising temperature further supports enhanced interaction strength and thermally favored adsorption on the heterogeneous hydrogel surface. The Temkin model revealed decreasing adsorption energy (B) and increasing binding constant (KT) with temperature, indicating an influence of thermal effects; however, its comparatively lower R^2 values limit its applicability. Overall, these results demonstrate that the Freundlich isotherm most accurately represents the adsorption of BG onto the nanocomposite, highlighting the role of surface heterogeneity and physisorption in governing the removal process [2, 28]

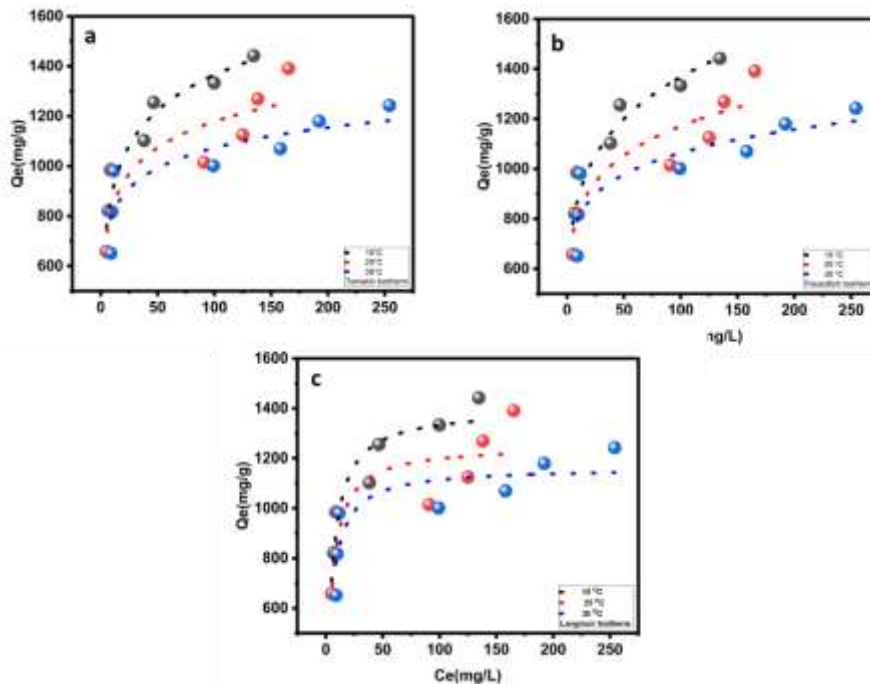


Figure 12. Nonlinear isotherms model for BG dye at different temperatures: (a) Temkin, (b) Freundlich, and (c) Langmuir

Table 1. Isotherm parameters and correlation coefficients for the Langmuir, Freundlich, and Temkin models for the adsorption of BG dye onto the hydrogel composite

Model	15°C	25°C	35°C
Langmuir			
KL	0.202	0.226	0.224
Qmax	1399.358	1251.172	1163.291
R ²	0.9203	0.7799	0.7432
Freundlich			
KF	573.122	577.583	605.916
N	5.205	6.514	8.184
R ²	0.9226	0.7613	0.7724
Temkin			
KT	7.764	24.059	39.722
B	205.141	151.382	117.342
R ²	0.9349	0.7974	0.7674

3.12. Kinetic studies

To elucidate the adsorption mechanism of BG dye onto the hydrogel composite, the experimental data were fitted to the pseudo-first-order and pseudo-second-order kinetic models. The objective was to determine the most suitable model for representing the experimental data, as shown in **Figure 13**. The pseudo-first-order model exhibited a poor correlation with the data, yielding a low coefficient of determination ($R^2 = 0.2232$). The calculated equilibrium adsorption capacity ($Q_e = 779.487\text{mg/g}$) was also significantly lower than the experimentally determined value (Q_e), indicating the inadequacy of this model to describe the adsorption behavior. In contrast, the pseudo-second-order model demonstrated an excellent fit with the experimental results. The R^2 value was high (0.9615), and the theoretical Q_e value (832.602 mg/g) was in close agreement with the actual experimental value. This confirms that the adsorption process is governed by a chemical mechanism involving interactions at the material's surface. These findings indicate that the pseudo-second-order kinetic model is the most appropriate for describing the BG adsorption process, which suggests that the rate-limiting step is chemisorption, occurring via chemical bonding rather than solely through physical forces^[29, 30]

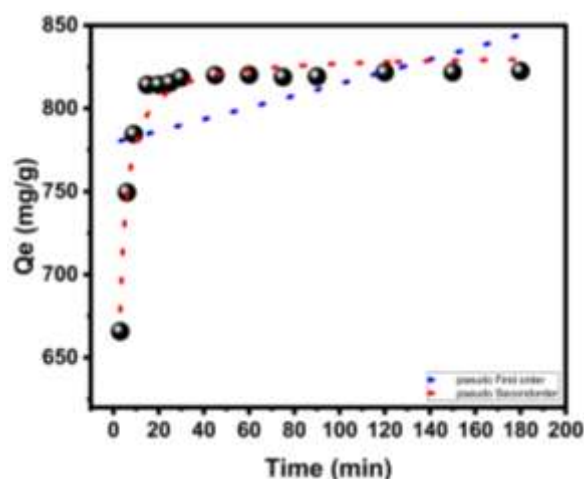


Figure 13. Nonlinear Kinetic models for BG dye onto the hydrogel composite

Table 2. Adsorption kinetics parameters for BG dye adsorption onto the hydrogel composite

Parameters	Pseudo-First Order	Pseudo-Second Order
K	4.44139×10^{-4}	0.017
Qe	779.487	832.602
R ²	0.2232	0.9615

3.13. Reusability study

The reusability of an adsorbent is a key parameter for assessing its practical and economic viability. As shown in Figure 14, the hydrogel composite retained high adsorption efficiency during the first three adsorption–desorption cycles, demonstrating the effectiveness of the regeneration process in restoring active sites. However, a gradual decline in performance was observed after the third cycle, with efficiency decreasing significantly by the fifth cycle. This reduction can be attributed to pore blockage by residual dye molecules and the partial loss of functional groups caused by repeated exposure to the regeneration medium (0.1 M HCl for 4 h). While acid washing effectively desorbs bound dye, it may also damage the polymeric structure over multiple cycles. To improve long-term stability, milder or alternative regeneration approaches—such as ethanol/water mixtures, dilute alkaline solutions, or salt-assisted desorption—could be explored, as these methods are less destructive to the functional groups while maintaining desorption efficiency. Overall, despite the observed decline after repeated use, the results confirm that the hydrogel composite exhibits strong reusability and remains a promising candidate for wastewater treatment applications [31, 32].

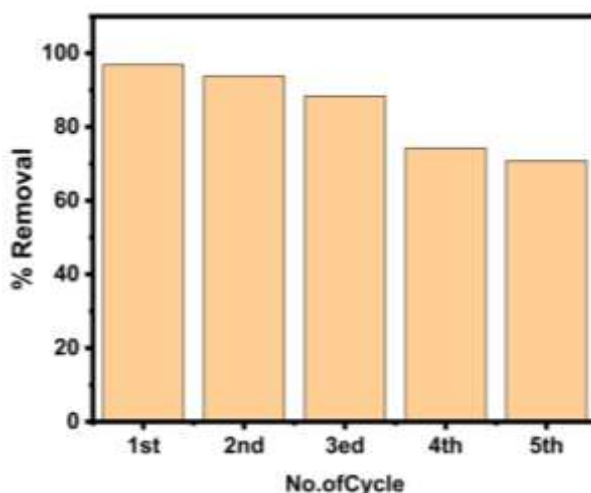


Figure 14. Reusability of hydrogel composite

4. Conclusion

This study demonstrated the effectiveness of the hydrogel composite in removal BG dye from aqueous solutions. Kinetic modeling revealed that the pseudo-second-order model best described the adsorption behavior. Among the isotherm models, Freundlich showed the highest correlation, reflecting multilayer adsorption on a heterogeneous surface. FTIR and SEM analyses confirmed that the incorporation of AC and enhanced porosity and improved surface morphology, which positively influenced adsorption efficiency. Both pH and temperature significantly affected performance, with optimal removal observed under alkaline conditions and at lower temperatures, suggesting an exothermic adsorption mechanism. Reusability showed that the hydrogel composite maintained its efficiency over three consecutive cycles, with a noticeable decline after the fourth cycle due to saturation of active sites. Based on these findings, the composite hydrogel is a promising material for dye-contaminated water treatment, owing to its enhanced physicochemical properties, regenerable performance, and suitability for sustainable industrial applications.

Conflict of interest

The authors declare no conflict of interest

References

1. Mahmood, A.A. and A.A. Hassan, Green synthesis of AC/ZnO nanocomposites for adsorptive removal of organic dyes from aqueous solution *Inorganic Chemistry Communications*, 2023. 157: p. 111415.

2. Radoor, S., S.K. Kassahun, and H. Kim, Selective adsorption of cationic dye by κ -carrageenan-potato starch bio-hydrogel: Kinetics, isotherm, and thermodynamic studies. *Int J Biol Macromol*, 2024. 281(Pt 2): p. 136377.
3. Radia, N.D., et al., Eco-friendly Synthesis of Hydrogel Nano-composites for Removal of Pollutants as a Model Rose Bengal Dye. *International Journal of Drug Delivery Technology*, 2022. 12(4): p. 1527-1530.
4. Rana, V.S. and N. Sharma, Adsorption profile of anionic and cationic dyes through Fe₃O₄ embedded oxidized Sterculia gum/Gelatin hybrid gel matrix. *International Journal of Biological Macromolecules*, 2023. 232: p. 123098: <https://doi.org/10.1016/j.ijbiomac.2022.12.317>.
5. Alzayd, A.A.M. and N.D. Radia, Novel pH-sensitive of organic composite (kc-g-poly(AAc-co-AAm)/bentonite), synthesis and characterization candidate as a carrier for controlled release system in vitro to some drugs. *Carbon Letters*, 2024. 34(1): p. 505-517: <https://doi.org/10.1007/s42823-023-00674-1>.
6. Rahul and R. Jindal, Efficient removal of toxic dyes malachite green and fuchsin acid from aqueous solutions using Pullulan/CMC hydrogel. *Polymer*, 2024. 307: p. 127203: <https://doi.org/10.1016/j.polymer.2024.127203>.
7. Shalah, L.A.M., et al., Screen the efficient growth of e.Coli to removal congo red dye by some modified media. *International Journal of Pharmaceutical Research*, 2019. 11(2).
8. Sharma, S., et al., Adsorption of cationic dyes onto carrageenan and itaconic acid-based superabsorbent hydrogel: Synthesis, characterization and isotherm analysis. *Journal of Hazardous Materials*, 2021. 421: p. 126729 :<https://doi.org/10.1016/j.jhazmat.2021.126729>.
9. Aljeboree, A.M., et al., Highly Reusable Nano Adsorbent Based on Clay-Incorporated Hydrogel Nanocomposite for Cationic Dye Adsorption. *Journal of Inorganic and Organometallic Polymers and Materials*, 2025. 35(2): p. 1165-1186 : <https://doi.org/10.1007/s10904-024-03344-5>.
10. Thamer, B.M., et al., Highly selective and reusable nanoadsorbent based on expansive clay-incorporated polymeric nanofibers for cationic dye adsorption in single and binary systems. *Journal of Water Process Engineering*, 2023. 54: p. 103918: <https://doi.org/10.1016/j.jwpe.2023.103918>.
11. Tyagi, R., D. Dangi, and P. Sharma, Optimization of Hazardous Malachite Green Dye Removal Process Using Double Derivatized Guar Gum Polymer: A Fractional Factorial L9 Approach. *Sustainable Chemistry for Climate Action*, 2024: p. 100043 :<https://doi.org/10.1016/j.scca.2024.100043>.
12. Ullah, N., et al., Preparation and dye adsorption properties of activated carbon/clay/sodium alginate composite hydrogel membranes. *RSC Advances*, 2024. 14(1): p. 211-221.
13. Wang, Z.K., et al., Natural-clay-reinforced hydrogel adsorbent: Rapid adsorption of heavy-metal ions and dyes from textile wastewater. *Water Environment Research*, 2022. 94.
14. Aljeboree, A.M., et al., Facile fabrication of a low-cost carboxymethyl cellulose–polyacrylamide composite for the highly efficient removal of cationic dye: optimization, kinetic and reusability. *Journal of the Iranian Chemical Society*, 2025. 22(1): p. 91-111.
15. Aljeboree, A.M., et al., Preparation of sodium alginate-based SA-g-poly(ITA-co-VBS)/RC hydrogel nanocomposites: And their application towards dye adsorption. *Arabian Journal of Chemistry*, 2024. 17(3): p. 105589: <https://doi.org/10.1016/j.arabjc.2023.105589>.
16. Shen, Y., B. Li, and Z. Zhang, Super-efficient removal and adsorption mechanism of anionic dyes from water by magnetic amino acid-functionalized diatomite/yttrium alginate hybrid beads as an eco-friendly composite. *Chemosphere*, 2023. 336: p. 139233: <https://doi.org/10.1016/j.chemosphere.2023.139233>.
17. Shirsath, S.R., et al., Ultrasonically prepared poly(acrylamide)-kaolin composite hydrogel for removal of crystal violet dye from wastewater. *Journal of Environmental Chemical Engineering*, 2015. 3(2): p. 1152-1162: <https://doi.org/10.1016/j.jece.2015.04.016>.
18. Shubha, J.P., et al., Facile green synthesis of semiconductive ZnO nanoparticles for photocatalytic degradation of dyes from the textile industry: A kinetic approach. *Journal of King Saud University - Science*, 2022. 34(5): p. 102047.
19. Radia, N.D., A.M. Aljeboree, and A.A.A. Mhammed, Enhanced removal of crystal violet from aqueous solution using carrageenan hydrogel nanocomposite/MWCNTs. *Inorganic Chemistry Communications*, 2024. 167: p. 112803: <https://doi.org/10.1016/j.inoche.2024.112803>.
20. Tainara, V., Samantha E. S., Artifon, C. T., Pâmela B. V., Valter A. B., Alexandre T. P., Chitosan-based hydrogels for the sorption of metals and dyes in water: isothermal, kinetic, and thermodynamic evaluations. *Colloid and Polymer Science*, 2021. 299: p. 649–662.
21. Saeed, A., M. Sharif, and M. Iqbal, Application potential of grapefruit peel as dye sorbent: Kinetics, equilibrium and mechanism of crystal violet adsorption. *Journal of Hazardous Materials*, 2010. 179(1): p. 564-572 :<https://doi.org/10.1016/j.jhazmat.2010.03.041>.
22. Thamer, B.M., F.A. Al-Aizari, and H.S. Abdo, Activated Carbon-Incorporated Tragacanth Gum Hydrogel Biocomposite: A Promising Adsorbent for Crystal Violet Dye Removal from Aqueous Solutions. *Gels*, 2023. 9(12).
23. Shah, S.S., B. Ramos, and A.C. Teixeira Adsorptive Removal of Methylene Blue Dye Using Biodegradable Superabsorbent Hydrogel Polymer Composite Incorporated with Activated Charcoal. *Water*, 2022. 14, DOI: 10.3390/w14203313.

24. Thamer, B.M., et al., In Situ Preparation of Novel Porous Nanocomposite Hydrogel as Effective Adsorbent for the Removal of Cationic Dyes from Polluted Water. *Polymers*, 2020. 12(12): p. 3002; <https://doi.org/10.3390/polym12123002>.
25. Taktak, F.F. and E. Özyaranlar, Semi-interpenetrating network based on xanthan gum-cl-2-(N-morpholinoethyl methacrylate)/titanium oxide for the single and binary removal of cationic dyes from water. *International Journal of Biological Macromolecules*, 2022. 221: p. 238-255; <https://doi.org/10.1016/j.ijbiomac.2022.08.139>.
26. Thakur, S., et al., Highly efficient poly(acrylic acid-co-aniline) grafted itaconic acid hydrogel: Application in water retention and adsorption of rhodamine B dye for a sustainable environment. *Chemosphere*, 2022. 303: p. 134917.
27. Aljeboree, A.M., et al., Synthesis and swelling behavior of highly adsorbent hydrogel for the removal of brilliant green from an aqueous solution: Thermodynamic, kinetic, and isotherm models. *Case Studies in Chemical and Environmental Engineering*, 2024. 10: p. 100831; <https://doi.org/10.1016/j.cscee.2024.100831>.
28. Aljeboree, A.M. and A.F. Alkaim, Studying removal of anionic dye by prepared highly adsorbent surface hydrogel nanocomposite as an applicable for aqueous solution. *Scientific Reports*, 2024. 14(1): p. 9102 : <https://doi.org/10.1038/s41598-024-59545-y>.
29. Al-Mashhadani, Z.I., et al., Antibiotics Removal by Adsorption onto Eco-friendly Surface: Characterization and Kinetic Study. *International Journal of Pharmaceutical Quality Assurance*, 2021. 12(4): p. 252-255.
30. Zoya, Z., A. Aisha, and S.A. Elham, Adsorption of methyl red on biogenic Ag@Fe nanocomposite adsorbent: Isotherms, kinetics and mechanisms. *Journal of Molecular Liquids*, 2019. 283: p. 287-298 :<https://doi.org/10.1016/j.molliq.2019.03.030>.
31. Xinyou, M., et al., Synthesis of a three-dimensional network sodium alginate–poly(acrylic acid)/attapulgate hydrogel with good mechanic property and reusability for efficient adsorption of Cu²⁺ and Pb²⁺. *Environmental Chemistry Letters*, 2018. 16: p. 653–658.
32. Bessaha, G., et al., Enhancement of the comprehensive performance of tetracycline adsorption by halloysite nanotubes: Kinetics, mechanism, and reusability study. *Desalination and Water Treatment*, 2024. 320: p. 100695.